J. Fluid Mech. (1975), *vol.* 67, *part* 2, *pp.* 273–288
Printed in Great Britain

On the correlation between temperature and velocity dissipation fields in a heated turbulent jet

By R. A. ANTONIA

Department of Mechanical Engineering, University of Sydney, New South Wales 2006

AND C. W. VAN ATTA

Department of Applied Mechanics and Engineering Sciences, University of California, San Diego

(Received 25 February 1974)

A few statistical properties of fine-scale velocity and temperature fluctuations have been measured on the axis of symmetry of a heated turbulent round jet. The probability density of $\partial\theta/\partial x$, the streamwise derivative of the temperature fluctuation, is strongly negatively skewed, indicating a lack of isotropy for the fine-scale temperature structure. An estimate of the correlation between the velocity and temperature dissipation fields has been obtained by assuming that the dissipation of velocity and dissipation of temperature can be approximated by $(\partial u/\partial x)^2$, where u is the streamwise velocity fluctuation, and $(\partial\theta/\partial x)^2$ respectively. The correlation between the quantities $(\partial u/\partial x)^2_r$ and $(\partial\theta/\partial x)^2_r$, averages over a volume of linear dimension r, is fairly high and depends on the choice of r. An analysis shows that this correlation plays a vital role in the prediction of high-order structure functions of u and θ. The assumed lognormality of the probability density of $(\partial u/\partial x)^2_r$ and $(\partial\theta/\partial x)^2_r$ and of their joint density is found to be reasonable over a range of r corresponding to the inertial subrange.

1. Introduction

The modification by Kolmogorov (1962) and Oboukhov (1962) of Kolmogorov's (1941) local isotropy and similarity hypotheses to allow for the fluctuations in ϵ, the rate of dissipation of turbulent energy, has led to a number of important consequences with regard to the small-scale properties of turbulence. Yaglom (1966) showed that the fluctuations in ϵ result in a change to a $k^{-1+\mu}$ behaviour for the spectrum of ϵ in the inertial wavenumber range (k is the wavenumber $2\pi f/U$, where f is the frequency and U the local mean velocity), where μ is a universal constant according to Kolmogorov's (1962) third hypothesis, and equal to about 0·5. Yaglom also showed that the fluctuations in ϵ lead to an inertial-subrange spectral shape of the streamwise velocity fluctuations u of $k^{-\frac{5}{3}-\frac{1}{9}\mu}$. The decrease in the exponent of k from its usually assumed value of $-\frac{5}{3}$ is clearly within the scatter of experimental data. Whilst the influence of ϵ fluctuations on second-order moments of the velocity u can be neglected, their influence on higher-order moments of $\partial u/\partial x$ can be exemplified by the strong Reynolds number dependence of experimental data on $(\partial u/\partial x)^3$ and $(\partial u/\partial x)^4$ (for a summary of the available experimental data see Kuo & Corrsin 1971).

Van Atta (1971) considered the influence of fluctuations in ϵ or χ, the dissipation of passive-scalar fluctuations, on turbulent scalar characteristics in the inertial subrange. He showed that these characteristics are not only influenced by ϵ and χ but also by the correlation between the two dissipation fields. Over a range of all possible values of this correlation, Van Atta showed that the inertial-subrange power law for the spectrum of scalar fluctuations would range from $k^{-1\cdot 39}$ to $k^{-1\cdot 72}$, a variation which is once again too small to be detected experimentally. There are no available experimental data on the correlation between χ and ϵ. The aim of the present work is to obtain a measure of this correlation on the axis of symmetry of a heated round jet, assuming that ϵ and χ can be approximated by $(\partial u/\partial x)^2$ and $(\partial \theta/\partial x)^2$ respectively (θ is the temperature fluctuation). The influence of the fluctuations of ϵ and χ on structure functions of velocity and temperature fluctuations in the inertial subrange is examined in § 4. Some of the assumptions made with regard to the statistical properties of ϵ_r and χ_r, the values of ϵ and χ averaged over a volume of linear dimension r, and of the product $\epsilon_r \chi_r$ have been experimentally tested (§ 5).

2. Experimental techniques and conditions

The time derivatives of velocity and temperature fluctuations were obtained simultaneously on the axis of symmetry of a heated turbulent round jet developing in a co-flowing external stream. A description of the heated-jet facility can be found in Antonia & Bilger (1973). At the exit from the nozzle (of diameter 15·9 mm) the temperature T_j and the velocity U_j of the jet were kept constant at 190 °C and 44 m s^{-1} respectively. The velocity U_1 of the external stream at the ambient laboratory temperature was in general 2·6 m s^{-1} but a few measurements were also made for $U_1 = 7\cdot 9$ m s^{-1}.

The velocity and temperature fluctuations u and θ were measured with two platinum-plated tungsten wires 5 μm in diameter placed in a parallel array on the same probe with the body of the probe aligned with the axis of the jet. The wire length was equal to 1·0 mm and the separation in the radial direction between the wires was 0·4 mm. One of the wires was operated as a 'cold' wire by the DISA 55M20 constant-current bridge of a DISA 55M01 anemometer system. The other wire was operated as a 'hot' wire with an overheat ratio of 0·8 on the DISA 55M10 constant-temperature bridge of a second DISA 55M01 anemometer system.

The cold wire was run at a current of 2 mA. At this current the sensitivity to velocity was found to be negligible. The signal from the constant-current bridge was compensated using a frequency compensator designed to maintain a flat frequency response up to 20 kHz (the time constant of the wire was typically 0·56 ms at 8 m s^{-1}). The compensated signal was subtracted from the hot-wire signal in a DISA 55D26 signal conditioner. Before subtraction, the temperature-contaminated velocity signal from the hot wire was fed into a variable-gain

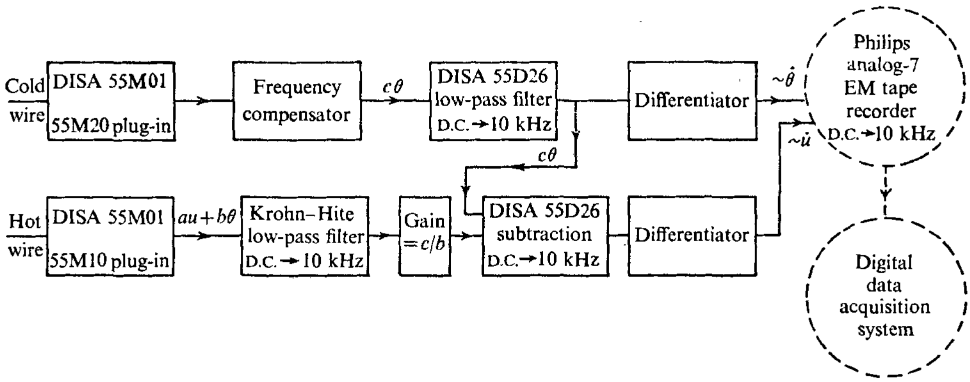

FIGURE 1. Block diagram of analog and digital processing.

amplifier, as shown in figure 1. The setting of this amplifier was determined by the temperature sensitivity of the hot-wire signal, inferred by calibration of the hot wire in the potential core of the heated jet. The calibration was carried out over a velocity and temperature range covering the experimental conditions. The two resulting signals (see figure 1), proportional to only either the velocity or temperature fluctuations, were then differentiated by identical differentiator circuits (with a linear frequency response up to 20 kHz and a fall-off of 6 db/octave on both sides of this peak). The differentiated signals were recorded on a Philips ANALOG-7 FM tape recorder at 76·2 mm s^{-1} (the frequency response of the tape recorder was checked to be flat up to 10 kHz). The recorded signals were played back at 190·5 mm s^{-1} and digitized to 11 bit accuracy at a frequency of 3 kHz per channel (real-time sampling frequency of 12 kHz). Prior to digitization, the signals were low-pass filtered using two closely matched filters with the cut-off frequency set at 1·5 kHz (a real-time frequency of 6 kHz). The 6 kHz cut-off setting was selected using the estimated Kolmogorov frequency of 5·4 kHz (see below) on the axis of symmetry of the jet at $x/d = 59$ (x is the distance from the nozzle and d is the nozzle diameter) for $U_j/U_1 = 16{\cdot}3$.

All of the results presented in §3 were obtained at $x/d = 59$, where

$$\langle u^2\rangle^{\frac{1}{2}}/U = 0{\cdot}16 \quad \text{and} \quad \langle \theta^2\rangle^{\frac{1}{2}}/T = 0{\cdot}07,$$

U and T (measured in °C) being the local mean velocity and temperature respectively. The Kolmogorov microscale η, defined as $(\nu^3/\langle\epsilon\rangle)^{\frac{1}{4}}$, where ν is the kinematic viscosity and $\langle\epsilon\rangle$ the dissipation of turbulent energy, is equal to 0·15 mm. The frequency corresponding to the η-scale convection past the wire is given by $U/2\pi\eta$ and is approximately 5·4 kHz. It should be noted that, although η is comparable with the distance between the wires, it is significantly smaller than the length l (1 mm) of the wires. The attenuation of the high frequency content of the u and θ spectra as a result of the relatively high value of l/η cannot be easily estimated but the correction of Wyngaard (1968), based on the assumption of isotropy, suggests that the attenuation can be as much as 30 % when $k_1\eta = 1$. The correction of Wyngaard (1971*a*) for the spatial resolution of a cold wire shows that, for the present value of l/η, the measured value of $\langle\chi\rangle$ could be underestimated by as much as 30 %.

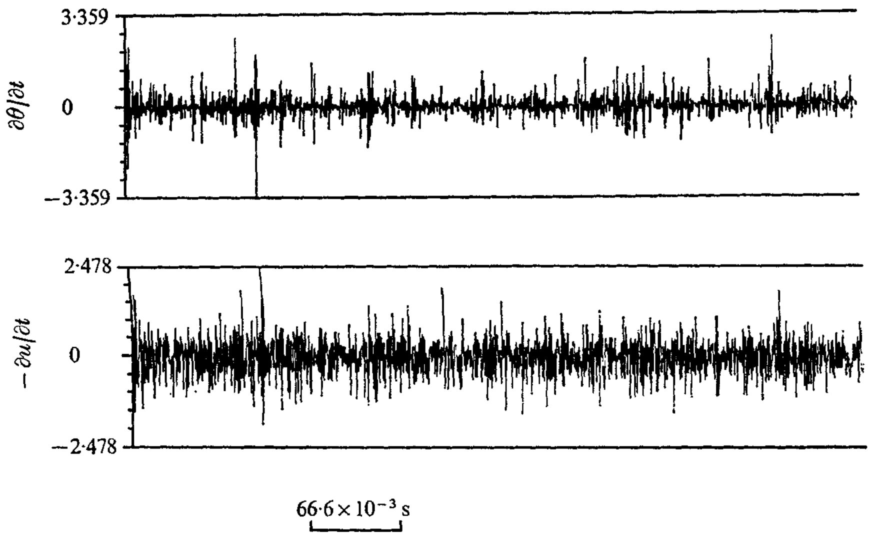

FIGURE 2. Records of simultaneous velocity and temperature derivatives (ordinate units are arbitrary).

3. Experimental results for $\partial\theta/\partial t$ and $\partial\theta/\partial t$

Computer plots of records of $\partial\theta/\partial t$ and $\partial u/\partial t$ at $x/d = 59$ shown in figure 2 reveal the more intermittent behaviour of $\partial\theta/\partial t$ in relation to that of the velocity derivative. The probability densities of $\partial\theta/\partial t$ and $\partial u/\partial t$ are given in figure 3 and are normalized such that the areas under the curves are equal to unity. Although the probability density $p(\partial u/\partial t)$ of $\partial u/\partial t$ deviates significantly from the Gaussian distribution, $p(\partial\theta/\partial t)$ shows even stronger departures from the normal curve near zero values of $\partial\theta/\partial t$. The skewness $S_{\dot{u}}$ of $\partial u/\partial t$, defined as

$$\langle(\partial u/\partial t)^3\rangle/\langle(\partial u/\partial t)^2\rangle^{\frac{3}{2}},$$

is 0·30 whilst the flatness factor $F_{\dot{u}} \equiv \langle(\partial u/\partial t)^4\rangle/\langle(\partial u/\partial t)^2\rangle^2$ is 6·4. The turbulence Reynolds number R_λ, defined as $\langle u^2\rangle^{\frac{1}{2}}\lambda/\nu$, where λ is the Taylor microscale ($\lambda^2 = \langle u^2\rangle/\langle(\partial u/\partial x)^2\rangle$), is 240. The value of $F_{\dot{u}}$ is in good agreement with that obtained by Kuo & Corrsin (1971) for a corresponding value of R_λ on the axis of an isothermal round jet issuing into still air. The magnitude of $S_{\dot{u}}$ is somewhat smaller than the mixing-layer value reported by Wyngaard & Tennekes (1970) but in reasonable agreement with the measurements of Antonia (1973) in the inner region of a boundary layer.

The flatness factor of $\partial\theta/\partial t$ is approximately 13·0, which agrees substantially with the R_λ trend of the available measurements of $F_{\dot{\theta}}$ reported in Antonia & Van Atta (1974). It should be noted that, although the values of F_{θ} are considerably higher than those of $F_{\dot{u}}$, the rate of increase of $F_{\dot{\theta}}$ with R_λ (Antonia & Van Atta) is only marginally higher than that for $F_{\dot{u}}$, as predicted in Kuo & Corrsin (1971), at least for R_λ greater than 300. For isotropic turbulence, the skewness of $\partial u/\partial x$ must be negative as $-\langle(\partial u/\partial x)^3\rangle$ represents a production rate

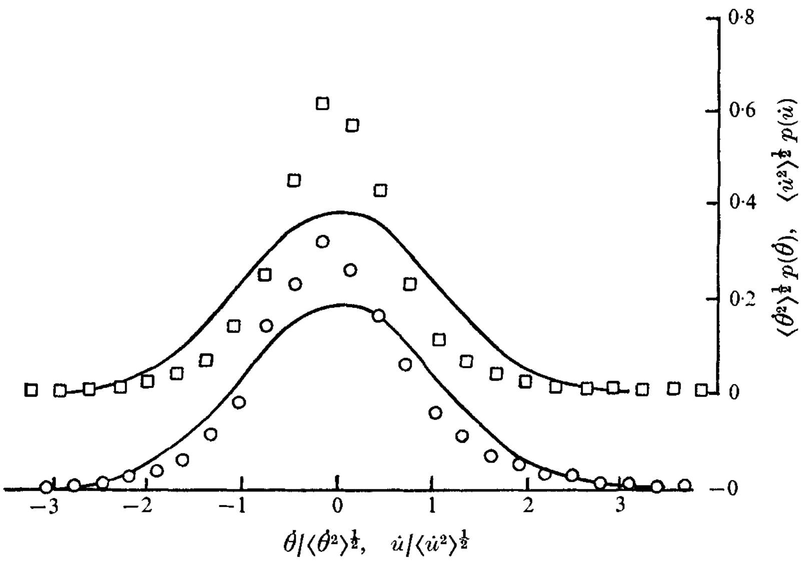

FIGURE 3. Probability density of velocity and temperature derivatives. □, $p(\dot{\theta})$; ○, $p(\dot{u})$; ——, Gaussian distribution.

of mean-square turbulent vorticity (cf. Saffman 1968; Wyngaard 1971*b*). The skewness of $\partial\theta/\partial x$ must be zero in isotropic turbulence to satisfy the requirement of invariance with respect to reflexion and rotation of the co-ordinate axes. For non-negligible velocity contamination of the cold wire, Wyngaard (1971*b*) shows that, again for isotropic turbulence, the measured value of $\langle(\partial\theta/\partial x)^3\rangle$ must be positive. The skewness of $\partial\theta/\partial x$ is equal to $-0{\cdot}7$. This value is in reasonable agreement with a measurement by Gibson & Masiello (1972) on the axis of a heated jet, but of opposite sign to the boundary-layer (Gibson, Stegen & Williams 1970) and wake (Freymuth & Uberoi 1971, 1973) measurements. Using the expression for the velocity sensitivity of a cold wire given by equation (29) in Wyngaard's (1971*b*) paper, the velocity sensitivity for the present wire operating conditions is estimated to be about 0·012 °C/m s^{-1}. This then leads to a velocity-induced skewness of $\partial\theta/\partial x$ of 0·014 (obtained using equation (22) in Wyngaard's paper), which is clearly negligible when compared with the measured value. Also, Wyngaard's analysis overestimates the skewness error, as it employs a correlation coefficient $S_T \equiv \langle(\partial\theta/\partial x)^2(\partial u/\partial x)\rangle/\langle(\partial\theta/\partial x)^2\rangle\langle(\partial u/\partial x)^2\rangle^{\frac{1}{2}}$ of $-2{\cdot}05$ whilst the measured value is $-0{\cdot}27$.†

The present value of $S_{\dot{\theta}}$ and the values reported in Freymuth & Uberoi (1973) tend to indicate a rather strong departure from local isotropy conditions on the axis of symmetry of both axisymmetric jets and wakes. Gibson, Friehe & McConnell (1973, private communication) have suggested that the local

† Clay (1973) obtained a value of $-0{\cdot}40$ for S_T when the streamwise separation between the velocity and scalar sensors was less than $0{\cdot}5\eta$, whilst S_T is close to zero when the separation is about 5η. The present magnitude of S_T is probably too high when the present radial separation 3η between the two wires is taken into account but it should also be noted (Van Atta 1974) that the magnitude of S_T may increase slightly with increasing R_λ.

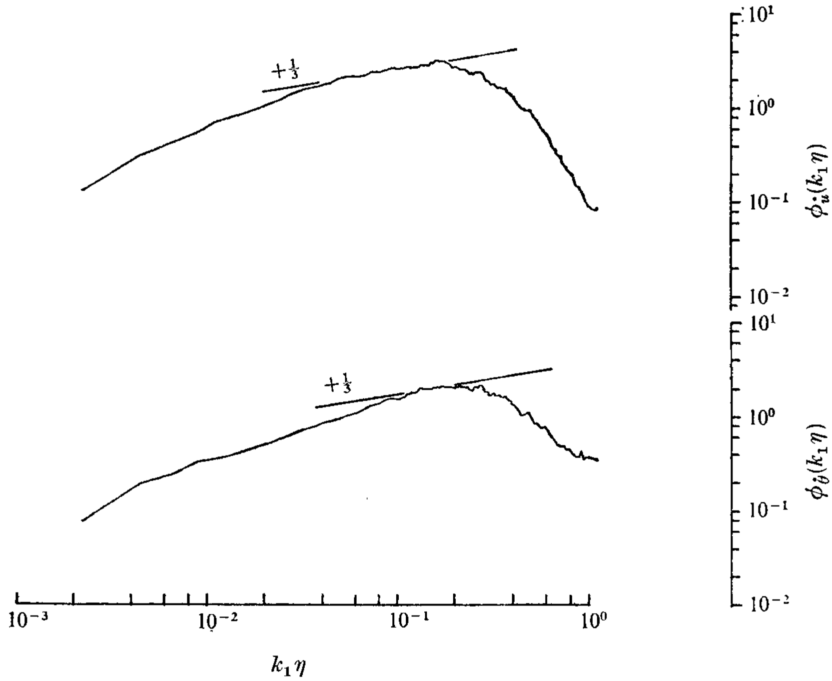

FIGURE 4. Spectra of $\dot{\theta}$ and $\dot{u}$.

anisotropy of the temperature field might be associated with temperature jumps occurring across a system of large eddies rolling with the mean vorticity of the shear flow. Evidence of this large-scale structure behaviour can be seen in the conditionally sampled temperature measurements of Fiedler (1974) in the two-dimensional mixing layer and of Antonia (1974) in the axisymmetric jet.

Figure 4 shows computer plots of the spectra of $\partial\theta/\partial t$ and $\partial u/\partial t$, which can be interpreted as dissipation spectra of the temperature and velocity fluctuations respectively. The spectra were obtained by applying the fast Fourier transform algorithm with a block length of 2048 samples and performing an ensemble average over 60 blocks. At the present sampling frequency of 12 kHz, this amounts to an overall sample duration of 10·24 s (this value was used for computing all the results presented in this paper). The standard deviation for each spectral estimate was found to be less than 15%. The variances of $\partial\theta/\partial t$ and $\partial u/\partial t$ for a given frequency band have been normalized by $\langle(\partial\theta/\partial t)^2\rangle$ and $\langle(\partial u/\partial t)^2\rangle$ and the scaling in figure 4 is such that

$$\int_0^\infty \phi_{\dot{\theta}}\, d(k_1\eta) = 1, \quad \int_0^\infty \phi_{\dot{u}}\, d(k_1\eta) = 1.$$

Both spectra peak near $k_1\eta = 0{\cdot}15$ but the extent of the inertial subrange in the $\partial u/\partial t$ spectrum ($\phi_{\dot{u}} \sim \langle\epsilon\rangle^{\frac{2}{3}} k_1^{\frac{1}{3}}$) is somewhat larger than that for $\partial\theta/\partial t$

$$(\phi_{\dot{\theta}} \sim \langle\chi\rangle\langle\epsilon\rangle^{-\frac{1}{3}} k_1^{\frac{1}{3}}).$$

4. Structure functions of velocity and temperature in the inertial subrange

The statistical properties of the velocity and temperature fluctuations of a scale comparable with the Kolmogorov microscale η are assumed to be a function of ν, the kinematic viscosity, α, the thermal diffusivity of the fluid, and χ_r and ϵ_r, the dissipation of temperature and dissipation of velocity fluctuations respectively averaged over a volume of linear dimension r. The averaging was included in the refined hypothesis of Kolmogorov (1962) to allow for the influence of the spatial or temporal fluctuations of ϵ on the behaviour of the small-scale velocity fluctuations. If we consider the quantities Δu and $\Delta\theta$, where

$$\Delta u = u(x+r,t) - u(x,t) \quad \text{and} \quad \Delta\theta = \theta(x+r,t) - \theta(x,t),$$

then, in general,

$$\langle(\Delta u)^m (\Delta\theta)^n\rangle_{\epsilon_r,\,\chi_r} = C_{mn}\,\nu^a\alpha^b r^c \epsilon_r^d \chi_r^e,$$

with the averaging performed over only fixed values of ϵ_r and χ_r (Oboukhov 1962; Van Atta 1971). Averaging over all occurrences of ϵ_r and χ_r gives

$$\langle(\Delta u)^m(\Delta\theta)^n\rangle = C_{mn}\,\nu^a\alpha^b r^c\langle\epsilon_r^d\chi_r^e\rangle. \tag{1}$$

Dimensional considerations yield $e = \frac{1}{2}n$, $c = n-m+4d$ and $a+b = m-3d-\frac{1}{2}n$. The C_{mn} are universal constants which depend on the values of m and n under consideration. In the inertial subrange, with $\eta \ll r \ll L$ (L is a length scale associated with the large-scale structure), the dependence on ν and α in (1) can be ignored (only fluids with Prandtl number ν/α near unity are considered here). A more general analysis for small r to obtain the dependence on the Prandtl number ν/α does not appear possible in this case, as the dimensional analysis gives only a relation containing an arbitrary function of the two variables r/η and $Pr \equiv \nu/\alpha$. With a and b set to zero, (1) becomes

$$\langle(\Delta u)^m(\Delta\theta)^n\rangle = C_{mn}\,r^{\frac{1}{3}(m+n)}\langle\epsilon_r^{\frac{1}{2}m-\frac{1}{6}n}\,\chi_r^{\frac{1}{2}n}\rangle. \tag{2}$$

In particular, the second-order velocity and temperature structure functions are given by

$$\langle(\Delta u)^2\rangle = C_{20}\,r^{\frac{2}{3}}\langle\epsilon_r\rangle^{\frac{2}{3}} \tag{3}$$

and

$$\langle(\Delta\theta)^2\rangle = C_{02}\,r^{\frac{2}{3}}\langle\epsilon^{-\frac{1}{3}}\chi_r\rangle. \tag{4}$$

Kolmogorov (1962) and Oboukhov (1962) assumed that ϵ_r is lognormally distributed. Van Atta (1971) assumed that both χ_r and ϵ_r are lognormally distributed and that their joint probability density is bivariate lognormal:

$$p(\chi_r,\epsilon_r) = [2\pi\chi_r\epsilon_r\sigma_1\sigma_2(1-\rho^2)^{\frac{1}{2}}]^{-1}$$
$$\times\exp\left\{\left[\left(\frac{\ln\chi_r - m_1}{\sigma_1}\right)^2 - \frac{2\rho}{\sigma_1\sigma_2}(\ln\chi_r - m_1)(\ln\epsilon_r - m_2) + \left(\frac{\ln\epsilon_r - m_2}{\sigma_2}\right)^2\right]\Big/2(1-\rho^2)\right\}, \tag{5†}$$

† This expression was used to compute the joint moments by Van Atta (1971), but owing to an oversight an incorrect form for $p(\chi_r,\epsilon_r)$ was referred to in that work.

where σ_1 and σ_2 are the standard deviations of $\ln \chi_r$ and $\ln \epsilon_r$ respectively, $m_1 = \langle \ln \chi_r \rangle$, $m_2 = \langle \ln \epsilon_r \rangle$, and ρ is the correlation coefficient,

$$\rho = \langle (\ln \chi_r - \langle \ln \chi_r \rangle)(\ln \epsilon_r - \langle \ln \epsilon_r \rangle)\rangle / \sigma_1 \sigma_2. \tag{6}$$

To relate σ_1 and σ_2 to r, it has further been assumed (Kolmogorov 1962; Oboukhov 1962; Van Atta 1971) that

$$\sigma_1^2 = A_\theta + \mu_\theta \ln (L/r), \quad \sigma_2^2 = A + \mu \ln (L/r), \tag{7 a, b}$$

where μ and μ_θ are universal constants, and A and A_θ are constants which may depend on the geometry of the flow (the values of A and A_θ would almost certainly appear to be affected by the choice of the length scale L). Assumptions (7) and the assumed lognormality of ϵ_r and χ_r are strictly valid for $L \gg r$, i.e. for fairly high values of the turbulence Reynolds number.

Using (5) and (7), the cross-moments $\langle \epsilon_r^m \chi_r^n \rangle$ can be written down (e.g. Van Atta 1971) with the further assumption that $A = A_\theta$ and $\mu = \mu_\theta$:

$$\left.\begin{aligned} \langle \epsilon_r^m \chi_r^n \rangle &= \langle \epsilon \rangle^m \langle \chi \rangle^n \exp (A\Omega)(L/r)^{\mu\Omega}, \\ \text{where} \qquad \Omega &= \tfrac{1}{2}n(n-1) + \tfrac{1}{2}m(m-1) + mn\rho. \end{aligned}\right\} \tag{8}$$

For $n = 0$, this reduces to $\langle \epsilon_r^m \rangle = \langle \epsilon \rangle^m \exp [\frac{1}{2}\sigma_2^2 m(m-1)]$ or

$$\langle \epsilon_r^m \rangle = \exp (m \langle \ln \epsilon_r \rangle + \tfrac{1}{2} m^2 \sigma_2^2). \tag{9}$$

The inertial-subrange expressions (3) and (4) can be written as

$$\langle (\Delta u)^2 \rangle = C_{20} r^{\frac{2}{3}} \langle \epsilon \rangle^{\frac{2}{3}} \exp (-\tfrac{1}{9}A)(L/r)^{-\frac{1}{9}\mu} \tag{10}$$

and

$$\langle (\Delta \theta)^2 \rangle = C_{02} r^{\frac{2}{3}} \langle \epsilon \rangle^{\frac{1}{3}} \langle \chi \rangle \exp [\tfrac{1}{3}A(\tfrac{2}{3} - \rho)](L/r)^{\frac{1}{3}\mu(\frac{2}{3}-\rho)}. \tag{11}$$

Expression (10) is the same as the expression $C\langle \epsilon \rangle^{\frac{2}{3}} r^{\frac{2}{3}} (L/r)^{-\frac{1}{9}\mu}$ derived by Yaglom (1966), where the coefficient $C \equiv C_{20} \exp (-\frac{1}{9}A)$ now depends on the macrostructure of the flow. The fourth-order moment $\langle (\Delta u)^2 (\Delta \theta)^2 \rangle$ is given by

$$\langle (\Delta u)^2 (\Delta \theta)^2 \rangle = C_{22} r^{\frac{4}{3}} \langle \epsilon \rangle^{\frac{1}{3}} \langle \chi \rangle \exp [\tfrac{1}{3}A(-\tfrac{1}{3} + \rho)](L/r)^{\frac{1}{3}\mu(-\frac{1}{3}+\rho)},$$

and in normalized form,

$$\frac{\langle (\Delta u)^2 (\Delta \theta)^2 \rangle}{\langle (\Delta u)^2 \rangle \langle (\Delta \theta)^2 \rangle} = \frac{C_{22}}{C_{20} C_{02}} \exp [\tfrac{2}{3}A(\rho - \tfrac{1}{3})] \left(\frac{L}{r}\right)^{\frac{2}{3}\mu(\rho-\frac{1}{3})}. \tag{12}$$

The third-order moment $\langle (\Delta u)(\Delta \theta)^2 \rangle$ is given by

$$\langle \Delta u (\Delta \theta)^2 \rangle = C_{12} r \langle \chi \rangle, \tag{13}$$

an expression derived by Yaglom (1949) with $C_{12} = -\frac{2}{3}$. The skewness

$$\frac{\langle \Delta u (\Delta \theta)^2 \rangle}{\langle (\Delta u)^2 \rangle^{\frac{1}{2}} \langle (\Delta \theta)^2 \rangle} = \frac{C_{12}}{C_{20}^{\frac{1}{2}} C_{02}} \exp [\tfrac{1}{3}A(\rho - \tfrac{1}{2})] \left(\frac{L}{r}\right)^{\frac{1}{3}\mu(\rho-\frac{1}{2})}. \tag{14}$$

To retrieve the often-cited $r^{\frac{2}{3}}$ dependence of the second-order scalar structure function (11), ρ is required to be equal to $\frac{2}{3}$ (as given by Van Atta 1971). For this value of ρ, expressions (12) and (14) are clearly not independent of r. The value of the correlation coefficient ρ and its possible dependence on r are therefore of some importance in determining the dependence on r of the higher-order moments of

Δu and $\Delta\theta$. The magnitude of some of the coefficients C_{mn} can be inferred from some of the measured moments of structure functions in the inertial subrange. The atmospheric results of Paquin & Pond (1971) suggest that $C_{20} \simeq 2{\cdot}0$ and $C_{02} \simeq 1{\cdot}6$ provided that A is of order unity and the coefficient ρ is not too different from $\frac{2}{3}$. The value of C_{12} can be derived less ambiguously as (13) involves neither A nor ρ. The data of Paquin & Pond yield $C_{12} = -\frac{2}{3}$. The coefficients C_{0n}, for odd values of n, should in principle be zero if the small-scale temperature fluctuations are assumed to be locally isotropic. This latter assumption is, however, as pointed out in § 3, clearly in error.

To obtain some idea of the Reynolds number dependence of expressions such as (10), (11) and (12), it is possible to set r equal to the Taylor microscale λ (at least when $L \gg \lambda \gg \eta$) and use the isotropic turbulence relation $L/\lambda = R_\lambda/15$,† where L is defined by the equation $\langle\epsilon\rangle = Cv^3/L$ (Batchelor 1953, p. 103), C being approximately equal to $1{\cdot}0$. A partial summary of the measured values of μ compiled by Gibson & Masiello (1972) for high-R_λ atmospheric turbulence suggests an average value of approximately $0{\cdot}5$. This leads to $\langle(\Delta u)^2\rangle \sim R_\lambda^{-\frac{1}{18}}$ and a R_λ dependence for expression (12), when $\rho = \frac{2}{3}$. Both of these dependences are probably too weak to be detected experimentally but the dependence of $\langle(\partial u/\partial x)^3\rangle$, $\langle(\partial u/\partial x)^4\rangle$ and $\langle(\partial\theta/\partial x)^4\rangle$ has received a good deal of attention, both experimentally and analytically.

5. Experimental results for $(\partial u/\partial t)^2$ and $(\partial\theta/\partial t)^2$

As mentioned in § 2, the statistics of the fine-scale velocity and temperature fields were derived from digital records of $\partial u/\partial t$ and $\partial\theta/\partial t$, the time interval Δt between consecutive samples being $0{\cdot}83 \times 10^{-4}$ s. To obtain a measure of the statistics of χ_r and ϵ_r, it is assumed here that these two quantities are represented by $(\partial\theta/\partial x)_r^2$ and $(\partial u/\partial x)_r^2$ respectively. This assumption is clearly open to doubt, even in the case of isotropic turbulence (cf. Gibson *et al.* 1970). The time separations Δt are converted to space separations using Taylor's hypothesis

$$\Delta x = -U\Delta t$$

and the averaging length r is then given by $r = i\Delta x$, where $i = 1, 2$, etc.

The dependence of ρ on r is shown in figure 5. In the inertial subrange, r/η is in the range 6–25. However, it should be cautioned that there exists a certain amount of vagueness in the definition of the limits of an inertial range and different kinds of measurements may be interpreted as defining different limits. For example, Van Atta & Chen (1970) found that measurements of second-order structure functions in atmospheric turbulence lead to a lower limit of the inertial subrange at about 50η. It seems natural to think that for very large Reynolds numbers ρ must be constant in the proper inertial subrange (although there is no strict proof of this statement) since the main contributions to ϵ and χ are associated with spatial length scales much smaller than those in the inertial range. At

† A more rigorous derivation of the Reynolds number dependence of the higher-order moments of the velocity and temperature derivatives can be found in Van Atta (1973) and Antonia & Van Atta (1974).

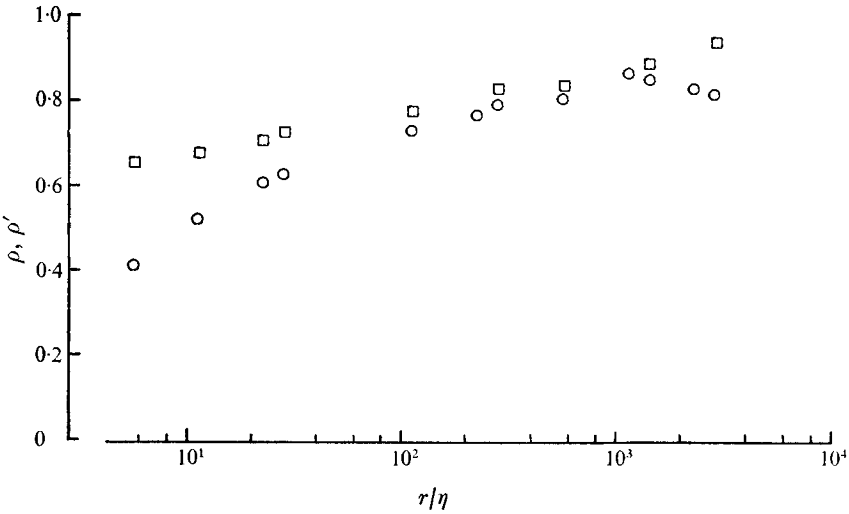

FIGURE 5. Correlation coefficients ρ and ρ' as functions of r.
□, ρ', equation (15); ○, ρ, equation (6).

the lower end of this range the values of ρ may have been affected by the wire length $l/\eta \simeq 6{\cdot}7$ but at the higher end of this range ρ continues to increase significantly. For $r/\eta > 800$, the results suggest that ρ reaches a constant value of about 0·84. Also shown in figure 5 is the correlation ρ' between $[(\partial u/\partial x)_r^2]$ and $[(\partial\theta/\partial x)_r^2]$, defined as

$$\rho' = \frac{\langle[(\partial\theta/\partial x)_r^2 - \langle(\partial\theta/\partial x)_r^2\rangle]\,[(\partial u/\partial x)_r^2 - \langle(\partial u/\partial x)_r^2\rangle]\rangle}{\sigma_1'\sigma_2'}, \tag{15}$$

where σ_1' and σ_2' are the standard deviations of $(\partial\theta/\partial x)_r^2$ and $(\partial u/\partial x)_r^2$ respectively. The coefficient ρ' appears to be proportional to $\ln r$ throughout the range of r considered here.

To test the assumption of lognormality of χ_r and ϵ_r and the lognormality of their joint probability density, some of the higher-order moments of

$$x \equiv \ln\chi_r - \langle\ln\chi_r\rangle \quad \text{and} \quad y \equiv \ln\epsilon_r - \langle\ln\epsilon_r\rangle$$

and of their product have been computed and are given in figures 6 and 7. As asserted by Oboukhov (1962), the assumption of lognormality is a reasonable approximation in that "the distribution of any essentially positive characteristic can be represented by a logarithmically Gaussian distribution with correct values of the first two moments". The third and fourth moments of x and y provide, however, a better indication of the suitability of the probability density. The skewnesses of x, y and $xy - \langle xy\rangle$ are given in figure 6. The skewness of x (defined as $\langle x^3\rangle/\langle x^2\rangle^{\frac{3}{2}}$) is essentially positive (except at the smallest value of r) with an average value of about 0·2. The skewness of y is negative but of similar magnitude to that of x. The product xy has an average skewness of about 2·2. Using the assumed normality of the joint probability density of x and y, the skewness of $xy - \langle xy\rangle$ is given by $2\rho(\rho^2+3)/(\rho^2+1)^{\frac{3}{2}}$ (cf. Antonia & Atkinson 1973). This distribution overpredicts the measured values except in the inertial subrange.

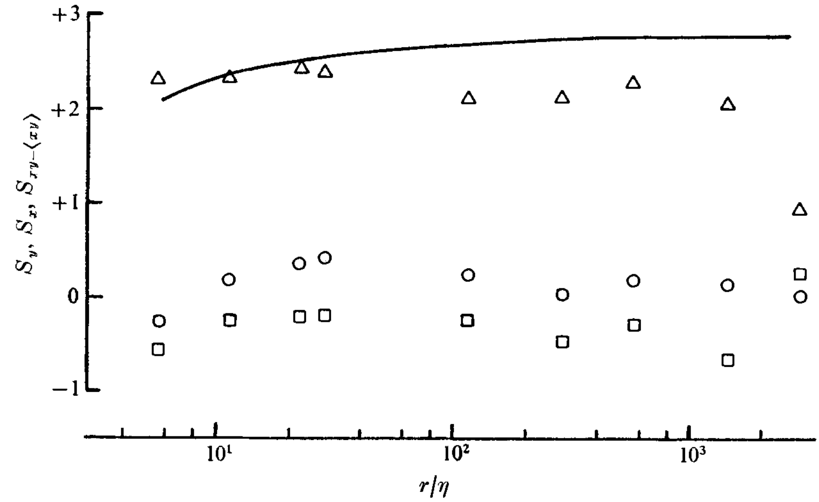

FIGURE 6. Skewness coefficients of $\ln(\partial\theta/\partial x)_r^2$, $\ln(\partial u/\partial x)_r^2$ and of their product. ○, S_x ($x \equiv \ln(\partial\theta/\partial x)_r^2 - \langle\ln(\partial\theta/\partial x)_r^2\rangle$); □, S_y ($y \equiv \ln(\partial u/\partial x)_r^2 - \langle\ln(\partial u/\partial x)_r^2\rangle$); △, $S_{xy-\langle xy\rangle}$; ——, $S_{xy-\langle xy\rangle} = 2\rho(\rho^2+3)/(\rho^2+1)^{\frac{3}{2}}$.

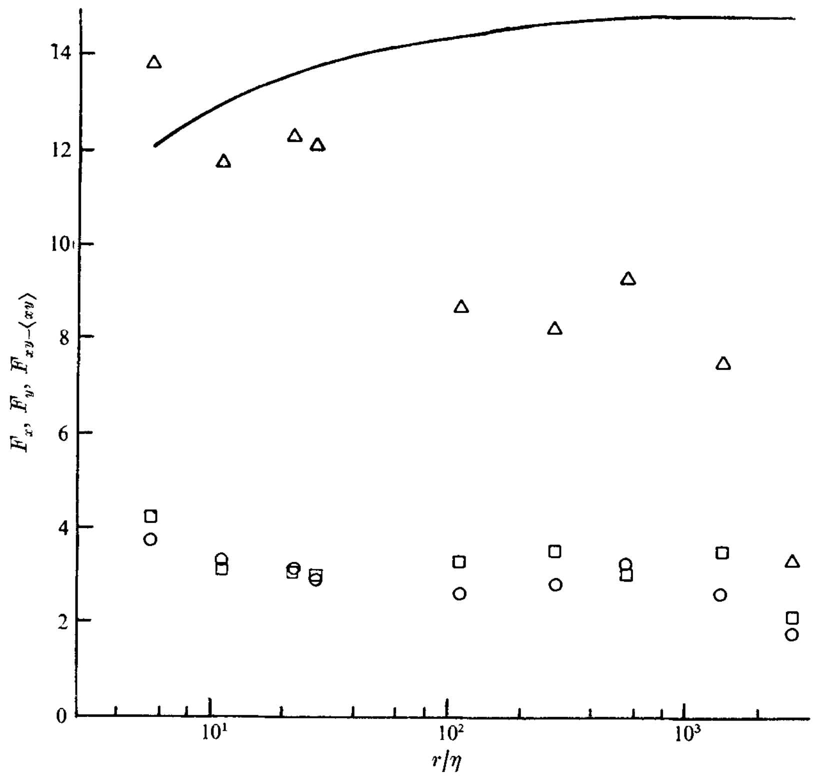

FIGURE 7. Flatness factors of $\ln(\partial\theta/\partial x)_r^2$, $\ln(\partial u/\partial x)_r^2$ and of their product. ○, F_x; □, F_y; △, $F_{xy-\langle xy\rangle}$; ——, $F_{xy-\langle xy\rangle} = (9\rho^4+42\rho^2+9)/(\rho^2+1)^2$.

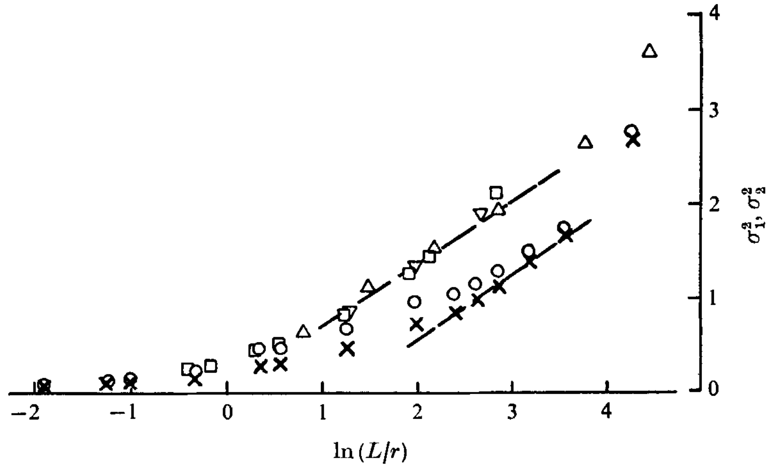

FIGURE 8. Variation with r of variance σ^2. ○, σ_1^2, $x/d = 59$, $U_j/U_1 = 16{\cdot}3$; △, σ_1^2, $x/d = 70$, $U_j/U_1 = 16{\cdot}3$; ▽, σ_1^2, $x/d = 59$, $U_j/U_1 = 5{\cdot}6$; □, σ_1^2, $x/d = 70$, $U_j/U_1 = 5{\cdot}6$; ×, σ_2^2, $x/d = 59$, $U_j/U_1 = 16{\cdot}3$.

The flatness factors of x and y (defined as $\langle x^4\rangle/\langle x^2\rangle^2$ and $\langle y^4\rangle/\langle y^2\rangle^2$ respectively), shown in figure 7, are not too different from the Gaussian value of 3·0 over most of the r/η range. The departure at the largest values of r probably cannot be trusted in view of the rather small number of samples used in obtaining these estimates. The flatness factor of $xy - \langle xy\rangle$ derived by using the Gaussian joint probability density is

$$(9\rho^4 + 42\rho^2 + 9)/(\rho^2+1)^2,$$

and is significantly higher than the measured values except once more for $r/\eta < 30$. It should be pointed out here that, as shown by Novikov (1971), although the lognormal distribution is a good asymptotic approximation, the moments need not tend towards the expressions resulting from the limiting distribution.

The verification of assumptions (7) is partially demonstrated by the results in figure 8, where the measured σ_1^2 and σ_2^2 are plotted against ln (L/r), where L is here, for convenience, derived from the isotropic relation for a jet, $L/\lambda = \frac{1}{15}R_\lambda$. The range of linear dependence of σ^2 on ln (L/r) is small and coincides approximately with the range of validity of the lognormal distributions. The values of μ and μ_θ are about 0·7 whilst A_θ is slightly larger than A. From measurements on the axis of a heated jet of large diameter, Masiello (1974) reports values of 0·45 and 0·84 for A_θ and A respectively whilst $\mu = 0{\cdot}47$ and $\mu_\theta = 0{\cdot}58$. The present asymptotic approach to zero of σ_1^2 and σ_2^2 as r becomes large is as expected and indicates that little significance can be given to the apparently good agreement of the flatness results of figure 9 for large values of r. Further support for the validity of (7a) with $\mu_\theta = 0{\cdot}7$ is provided by a few other results for σ_1^2 (figure 8) for different x/d and U_j/U_1. It is difficult to comment at present on the apparently lower value of A_θ for $x/d = 59$ ($U_j/U_1 = 16{\cdot}3$) in view of the uncertainty associated with the estimation of the length scale L. The flatness factors F_1 and F_2 defined as

$$F_1 = \langle[(\partial\theta/\partial x)_r^2]^2\rangle/\langle(\partial\theta/\partial x)_r^2\rangle^2 \quad \text{and} \quad F_2 = \langle[(\partial u/\partial x)_r^2]^2\rangle/\langle(\partial u/\partial x)^2\rangle^2$$

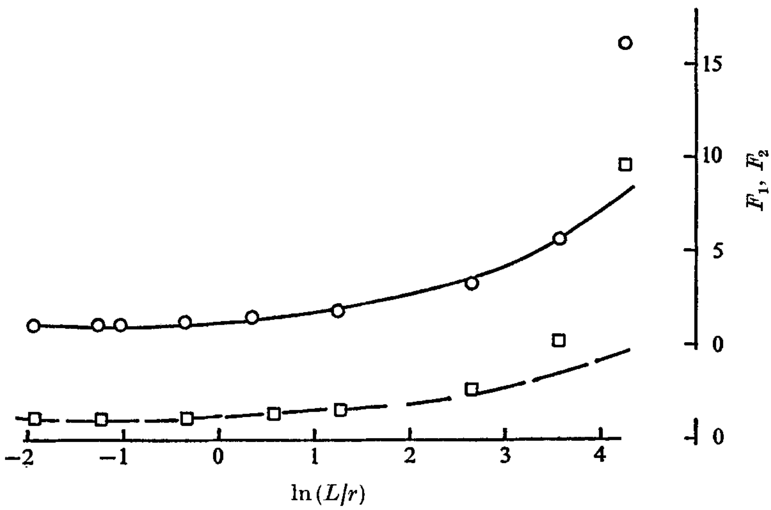

FIGURE 9. Comparison of flatness factors F_1 and F_2 with calculations using the lognormal distribution. ——, $F_1 = \langle((\partial\theta/\partial x)_r^2)^2\rangle/\langle(\partial\theta/\partial x)_r^2\rangle^2$; ○, $F_1 = \exp\sigma_1^2$; — —, $F_2 = \langle((\partial u/\partial x_r^2)^2\rangle/\langle(\partial u/\partial x)_r^2\rangle^2$; □, $F_2 = \exp\sigma_2^2$.

should become equal to the flatness factors of $\partial\theta/\partial x$ and $\partial u/\partial x$ respectively as r approaches η. Using (9), it follows that $F_1 = \exp\sigma_1^2$ and $F_2 = \exp\sigma_2^2$. The calculated F_1 and F_2 are compared with the measured values in figure 9. The agreement is good except at the lowest values of r/η, where the inferred values of F_1 and F_2 are significantly higher than the measured values. Note that, at $r/\eta \simeq 6$, the measured values of F_1 and F_2 are well below the magnitudes of the flatness factors of the unaveraged derivatives, i.e.

$$\langle(\partial\theta/\partial x)^4\rangle/\langle(\partial\theta/\partial x)^2\rangle^2 \quad \text{and} \quad \langle(\partial u/\partial x)^4\rangle/\langle(\partial u/\partial x)^2\rangle^2.$$

Indirect support for the present value of μ or μ_θ is available from the spectral densities of the fluctuations of $(\partial\theta/\partial t)^2$ and $(\partial u/\partial t)^2$ relative to their respective mean values. The spectra of figure 10 have been normalized so that

$$\int_0^\infty \phi_{\dot\theta^2}(k_1\eta)\,d(k_1\eta) = 1, \quad \int_0^\infty \phi_{\dot u^2}(k_1\eta)\,d(k_1\eta) = 1.$$

The shapes of the two spectra are closely similar and in the inertial subrange the slopes of $\phi_{\dot\theta^2}$ and $\phi_{\dot u^2}$ are reasonably approximated by $-\frac{1}{3}$. Note that, for $k_1\eta > 0{\cdot}1$, there is a significant increase in the spectral densities of $\dot u^2$ and $\dot\theta^2$. This increase is also present in the $\phi_{\dot u^2}$ spectrum for the jet data of Friehe, Van Atta & Gibson (1972) and the atmospheric data of Wyngaard & Pao (1972). Yaglom (1966) has predicted that, in the inertial subrange, the spectrum of the dissipation fluctuations is given by $k^{-1+\mu}$. Provided that the one-dimensional spectra of $\dot u^2$ and $\dot\theta^2$ can be loosely interpreted as the spectra of dissipation fluctuations of velocity and temperature respectively, it follows that $\mu_\theta = \mu = \frac{2}{3}$, in reasonable agreement with the value of 0·7 inferred from figure 9. As mentioned previously most of the estimates of μ for high-R_λ atmospheric turbulence data suggest a value close to 0·5. A spectrum of $(\partial u/\partial t)^2$ measured by Wyngaard & Tennekes

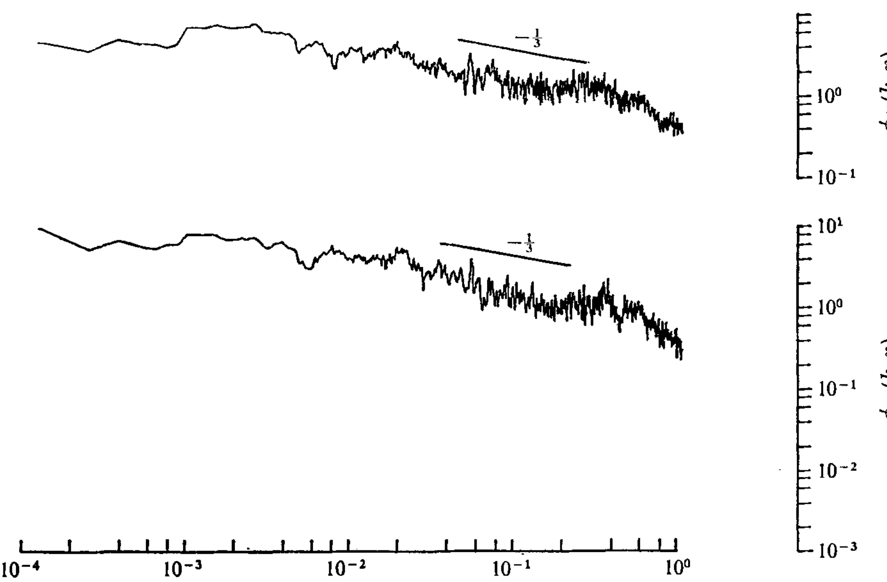

FIGURE 10. Spectra of $\dot{\theta}^2$ and $\dot{u}^2$.

(1970) in a curved mixing layer ($R_\lambda = 200$) gives $\eta = 0{\cdot}85$ whilst the spectrum of $(\partial u/\partial t)^2$ obtained by Friehe *et al.* (1972) on the axis of a round jet ($R_\lambda \simeq 540$) gives $\mu \simeq 0{\cdot}5$.

6. Conclusions

The experimental results of §§3 and 5 indicate a fairly strong correlation between $(\partial u/\partial x)_r^2$ and $(\partial\theta/\partial x)_r^2$. The normalized correlation coefficient

$$\langle(\partial u/\partial x)_r^2\,(\partial\theta/\partial x)_r^2\rangle/\langle(\partial u/\partial x)_r^2\rangle\,\langle(\partial\theta/\partial x)_r^2\rangle$$

is as high as $0{\cdot}7$ in a range of r coinciding with the inertial subrange of velocity and temperature fluctuations.

The assumed lognormality for $(\partial u/\partial x)_r^2$ and $(\partial\theta/\partial x)_r^2$ can only be considered as reasonable for values of r/η less than 30, in view of the relatively moderate Reynolds number of the present experiment and the, as yet unsupported, assumption that $(\partial u/\partial x)_r^2$ and $(\partial\theta/\partial x)_r^2$ are close approximations to ϵ_r and χ_r respectively. Gibson *et al.* (1970) have suggested that the approximation $\chi_r \sim (\partial\theta/\partial x)_r^2$ may be better than $\epsilon_r \sim (\partial u/\partial x)_r^2$ but the present results indicate that the deviation of the probability density of $\ln(\partial\theta/\partial x)_r^2$ from the Gaussian distribution can be as large as that for $\ln(\partial u/\partial x)_r^2$. The skewness of

$$\ln(\partial\theta/\partial x)_r^2 - \langle\ln(\partial\theta/\partial x)_r^2\rangle$$

is positive whilst that of

$$\ln(\partial u/\partial x)_r^2 - \langle\ln(\partial u/\partial x)_r^2\rangle$$

is negative for the whole range of values of r considered. The assumed lognormality for the probability density of the product $(\partial u/\partial x)_r^2(\partial\theta/\partial x)_r^2$ is also reasonable for r/η less than about 30. It should be re-emphasized that the present results obtained near $r/\eta \simeq 10$ must be treated with caution as the wire length was approximately $6{\cdot}7\eta$.

The variance relations (7) have also been verified over a range for r/η coinciding with reasonable lognormality of $(\partial u/\partial x)_r^2$ and $(\partial\theta/\partial x)_r^2$. In particular, the assumption that $\mu = \mu_\theta$ appears satisfactory and the present measured value of μ is about 0·7, which is somewhat higher than the value of 0·5 often quoted for atmospheric data. The data also suggest that $A \simeq A_\theta$ but the magnitude of A and its possible dependence on the nature and geometry of the flow are yet to be ascertained.

The correlation coefficient ρ [equation (6)] introduced by Van Atta (1971) is not constant in the inertial subrange but increases from about 0·5 to 0·7. This dependence on r, if true also for the true variables ϵ_r and χ_r, could change the rather simple predictions for the structure functions of velocity and temperature fluctuations presented in §4. The analysis given in §4 showed that a unique value of ρ could not satisfy the $r^{\frac{2}{3}}$ dependence of the structure function $\langle(\Delta\theta)^2\rangle$ of the temperature and the often-assumed independence of r of the cross-moments of Δu and $\Delta\theta$, such as given by the skewness in (14). It is strongly recommended that further measurements of ρ be made in high-R_λ flows, preferably in the atmospheric surface layer above land or water, where velocity and temperature fluctuations usually occur together and where the limitation of spatial resolution of the wire is less critical than for laboratory flows.

The work described here represents part of a programme of research supported by the Australian Research Grants Committee and the Australian Institute of Nuclear Science and Engineering. At UCSD, the work of C.V.A. was supported by N.S.F. Grant GK-43643X and by the Advanced Research Projects Agency of the Department of Defence, monitored by the U.S. Army Research Office under Contract DAHC 04-72-G0037.

REFERENCES

Antonia, R. A. 1973 Some small scale properties of boundary layer turbulence. *Phys. Fluids*, **16**, 1198.

Antonia, R. A. 1974 The distribution of temperature in the intermittent region of a turbulent shear flow. *Proc. 5th Int. Heat Transfer Conf., Tokyo*, vol. 2, p. 92.

Antonia, R. A. & Atkinson, J. D. 1973 High-order moments of Reynolds shear stress fluctuations in a turbulent boundary layer. *J. Fluid Mech.* **58**, 581.

Antonia, R. A. & Bilger, R. W. 1973 An experimental investigation of an axisymmetric jet in a co-flowing air stream. *J. Fluid Mech.* **61**, 805.

Antonia, R. A. & Van Atta, C. W. 1974 Prediction of high-order moments of turbulent temperature derivatives for large Reynolds numbers. *Phys. Fluids* (in press).

Batchelor, G. K. 1953 *The Theory of Homogeneous Turbulence*. Cambridge University Press.

Clay, J. P. 1973 Turbulent mixing of temperature in water, air and mercury. Ph.D. thesis, University of California, San Diego.

Fiedler, H. 1974 Transport of heat across a plane turbulent mixing layer. *Adv. in Geophys.* (in press).

Freymuth, P. & Uberoi, M. S. 1971 Structure of temperature fluctuations in the turbulent wake behind a heated cylinder. *Phys. Fluids*, **14**, 2574.

FREYMUTH, P. & UBEROI, M. S. 1973 Temperature fluctuations in the turbulent wake behind an optically heated sphere. *Phys. Fluids*, **16**, 161.

FRIEHE, C., VAN ATTA, C. W. & GIBSON, C. 1972 Jet turbulence dissipation rate measurements and correlations. *AGARD Current Paper*, no. 93, 18–1.

GIBSON, C. H. & MASIELLO, P. 1972 Observations of the variability of dissipation rates of turbulent velocity and temperature fields. In *Statistical Models and Turbulence. Lecture Notes in Physics*, vol. 12 (ed. M. Rosenblatt & C. Van Atta), p. 427. Springer.

GIBSON, C. H., STEGEN, G. R. & WILLIAMS, R. B. 1970 Statistics of the fine structure of turbulent velocity and temperature fields measured at high Reynolds number. *J. Fluid Mech.* **41**, 153.

KOLMOGOROV, A. N. 1941 The local structure of turbulence in an incompressible fluid for very large Reynolds numbers. *Dokl. Akad. Nauk. S.S.S.R.* **30**, 301.

KOLMOGOROV, A. N. 1962 A refinement of previous hypotheses concerning the local structure of turbulence in a viscous incompressible fluid at high Reynolds number. *J. Fluid Mech.* **13**, 82.

KUO, A. Y. & CORRSIN, S. 1971 Experiments on internal intermittency and fine-structure distribution functions in fully turbulent fluid. *J. Fluid Mech.* **50**, 285.

MASIELLO, P. J. 1974 Intermittency of the fine structure of turbulent velocity and temperature fields measured at high Reynolds number. Ph.D. thesis, University of California, San Diego.

NOVIKOV, E. A. 1971 Intermittency and scale similarity in the structure of a turbulent flow. *Prikl. Math. Mech.* **35**, 266.

OBOUKHOV, A. M. 1962 Some specific features of atmospheric turbulence. *J. Fluid Mech.* **13**, 77.

PAQUIN, J. E. & POND, S. 1971 The determination of the Kolmogoroff constants for velocity, temperature and humidity fluctuations from second- and third-order structure functions. *J. Fluid Mech.* **50**, 257.

SAFFMAN, P. G. 1968 Lectures on homogeneous turbulence. In *Topics in Non-Linear Physics* (ed. N. Zabusky), p. 485. Springer.

VAN ATTA, C. W. 1971 Influence of fluctuations in local dissipation rates on turbulent scalar characteristics in the inertial subrange. *Phys. Fluids*, **14**, 1803.

VAN ATTA, C. W. 1973 On the moments of turbulent velocity derivatives for large Reynolds numbers. *Charles Kolling Res. Lab., Dept. Mech. Engng, University of Sydney, Tech. Note*, F-49.

VAN ATTA, C. W. 1974 Influence of fluctuations in dissipation rates on some statistical properties of turbulent scalar fields. *Izv. Atmos. Ocean. Phys.* **7** (in press).

VAN ATTA, C. W. & CHEN, W. Y. 1970 Structure functions of turbulence in the atmospheric boundary layer over the ocean. *J. Fluid Mech.* **44**, 145.

WYNGAARD, J. C. 1968 Measurements of small-scale turbulence structure with hot wires. *J. Sci. Instrum., J. Phys.* E **1**, 1105.

WYNGAARD, J. C. 1971*a* Spatial resolution of a resistance wire temperature sensor. *Phys. Fluids*, **14**, 2052.

WYNGAARD, J. C. 1971*b* The effect of velocity sensitivity on temperature derivative statistics in isotropic turbulence. *J. Fluid Mech.* **48**, 763.

WYNGAARD, J. C. & PAO, Y. H. 1972 Some measurements of the fine structure of large Reynolds number turbulence. In *Statistical Models and Turbulence. Lecture Notes in Physics*, vol. 12 (ed. M. Rosenblatt & C. Van Atta), p. 384. Springer.

WYNGAARD, J. C. & TENNEKES, H. 1970 Measurements of the small-scale structure of turbulence at moderate Reynolds numbers. *Phys. Fluids*, **13**, 1962.

YAGLOM, A. M. 1949 On the local structure of the temperature field in a turbulent flow. *Dokl. Akad. Nauk. S.S.S.R.* **69**, 743.

YAGLOM, A. M. 1966 The influence of fluctuations in energy dissipation on the shape of turbulence characteristics in the inertial interval. *Sov. Phys. Dokl.* **11**, 26.